BAMS Article

The South American Tropopause Aerosol Layer (SATAL)

Caroline Bresciani, Dirceu Luis Herdies, Silvio Nilo Figueroa, Virginie Buchard, Arlindo M. da Silva, Charles Jones, and Leila M. V. Carvalho

KEYWORDS:
Reanalysis data;
Numerical analysis/modeling;
Seasonal variability;
Tropical variability;
Aerosols/particulates;
Atmospheric composition

ABSTRACT: The presence of an aerosol layer in the upper troposphere/lower stratosphere (UT/LS) in South America was identified with the Modern-Era Retrospective Analysis for Research and Applications version 2 (MERRA-2). This layer, which we shall refer to as the South American tropopause aerosol layer (SATAL), was identified over the Amazon basin at altitudes between 11 and 14 km. It exhibits a seasonal behavior similar to the Asian tropopause aerosol layer (ATAL) and the North American tropopause aerosol layer (NATAL). The SATAL is observed from October to March, coinciding with the presence of the South American monsoon. It forms first in the eastern Amazon basin in October, then moves to the southern Amazon, where it weakens in December–January and finally dissipates in February–March. We hypothesize that two main factors influence the SATAL formation in the UT/LS: 1) the source of aerosols from Africa and 2) the updraft mass flux from deep convective systems during the active phase of the South American monsoon system that transports aerosols to the UT/LS. Further satellite observations of aerosols and field campaigns are needed to provide useful information to find the origin and composition of the aerosols in the UT/LS during the South American monsoon.

SIGNIFICANCE STATEMENT: The purpose of this study is to better understand an increase in aerosol concentration in the upper troposphere/lower stratosphere (UT/LS) in South America. This is important because the atmospheric aerosol influences the Earth's radiative balance and climate and changes the temperature and precipitation cycles. Besides that, the aerosol in the UT/LS could be an aerosol source for remote regions and contribute to cloud formation. Our results suggest that an aerosol layer forms in the UT/LS during the summer months over South America, as soon as the region's rainy season begins.

https://doi.org/10.1175/BAMS-D-23-0074.1
Corresponding author: Dirceu Luis Herdies, dirceu.herdies@inpe.br
In final form 18 November 2023

AFFILIATIONS: Bresciani, Herdies, and Figueroa—National Institute for Space Research (INPE), Cachoeira Paulista, São Paulo, Brazil; **da Silva**—NASA Goddard Space Flight Center, Greenbelt, Maryland; **Buchard**—NASA Goddard Space Flight Center, Greenbelt, and GESTARII, University of Maryland, Baltimore County, Baltimore, Maryland; **Jones and Carvalho**—Department of Geography, and Earth Research Institute, University of California, Santa Barbara, Santa Barbara, California

Atmospheric aerosol particles play a key role in the Earth's radiative balance and climate by scattering and absorbing shortwave and longwave radiation and altering cloud properties (albedo and cloud microphysics). They act as cloud condensation nuclei (CCN) and interact directly and indirectly with solar radiation, absorbing or reflecting; changing the atmosphere temperature; and influencing the initiation of precipitation, visibility, and air quality (Myhre et al. 2013; Seinfeld and Pandis 2016; Twomey 1977). Aerosols present in the upper troposphere/lower stratosphere (UT/LS) are either primary aerosols transported from the lower troposphere to the UT/LS, or they are secondary aerosols resulting from new particle formation (Wang and Penner 2009; Yu and Luo 2009; Pierce and Adams 2009) associated with trace gases that have been transported to the UT/LS. If the particles grow by condensation and coagulation they can act as CCN in these remote regions (Merikanto et al. 2009). In the tropics, particles in the UT have been one of the largest aerosol reservoirs in the atmosphere. They may originate from primary aerosols, such as dust, organic carbon, and black carbon, or secondary aerosols formed by trace gases in the free troposphere.

Atmospheric aerosols and the new particle formation process have been the focus of numerous studies and field campaigns. Vernier et al. (2011) analyzed Cloud–Aerosol Lidar with Orthogonal Polarization (CALIOP) data to identify elevated aerosol layers in Asia. In this study, Vernier et al. showed the detection of the Asian tropopause aerosol layer (ATAL), which extends from the eastern Mediterranean to western China from 13 to 18 km of altitude during June–August. They used the scattering ratio from CALIOP and showed values of scattering ratio between 1.10 and 1.15 on average in the ATAL region during 3 of the 4 years analyzed. Due to volcanic activity, concentrations during 2009 were higher than in the other analyzed years. The authors suggested that the ATAL forms from the upward transport of primary aerosol by convection associated with the Asian monsoon.

Similarly, an aerosol layer has been observed over the southwestern United States and Mexico UT/LS (the North American tropopause aerosol layer, NATAL), which appears associated with the North American monsoon system (Vernier et al. 2011; Thomason and Vernier 2013). The NATAL is weaker than the ATAL and is mainly composed of biogenic secondary organic aerosol, whereas the ATAL is composed of sulfate and primary and secondary organic aerosol (Yu et al. 2015; Lau et al. 2018). Over South America, a large concentration of nanoparticles between 8 and 15 km altitude in the upper troposphere of the Amazon basin was identified with aircraft during the GoAmazon2014/5 field campaign (Martin et al. 2016; Wendisch et al. 2016). These particles differ in composition from the planetary boundary layer particles, suggesting that they are secondary aerosols (Andreae et al. 2018).

These observational studies motivated further investigation of the presence of a tropopause aerosol layer over South America similar to ATAL and NATAL that could be associated with the South American monsoon system (SAMS). The SAMS is characterized by significant

changes in atmospheric circulation and intense convective activity from winter to the summer austral season. The climatological onset of the SAMS wet season is in October, whereas the mature phase is in December–February and the demise in March–April (Zhou and Lau 1998; da Silva and de Carvalho 2007; Vera et al. 2006; Coelho et al. 2022).

The SAMS has unique features when compared with other monsoon systems. For instance, the SAMS is not associated with a seasonal wind reversal; rather, low-level winds are predominantly from the north-northeasterly direction over most of the tropical continent throughout the year (Zhou and Lau 1998). The South Atlantic convergence zone (SACZ), which is characterized by a convective band extending from the southern Amazon toward the subtropical western Atlantic, is another important component of the SAMS (Kodama 1992; Carvalho et al. 2004). The South American low-level jet (SALLJ), often observed east of the Andes, plays a significant role in transporting moisture from the tropics to the subtropics and in modulating the SAMS activity (Salio et al. 2002; Marengo et al. 2004; Wang and Fu 2004; Herdies et al. 2007; Montini et al. 2019). The upper-level Bolivian high, which is linked to the development of deep convection over tropical South America, is another relevant component of the SAMS. It is a large-scale anticyclonic system located, on average, over the Bolivian Altiplano that intensifies during the summer. The presence of this system is strikeout due to intense convection in the Amazon and flux of latent and sensible heat (Vera et al. 2006; Silva and Kousky 2012; Marengo et al. 2012).

The existence of intense convective activity over the Amazon basin and primary sources of aerosols, such as biogenic emissions, dust from the Sahara Desert, and emissions from burning biomass transported from Africa to South America (Andreae et al. 1990; Artaxo et al. 1990; Yáñez-Serrano et al. 2020; Holanda et al. 2020), suggest the existence of a tropopause aerosol layer over the Amazon basin. The main goal of this study is to investigate the presence of an aerosol layer in the UT/LS over the Amazon basin, hereafter referred to as the South American tropopause aerosol layer (SATAL).

Given the importance of aerosols in controlling Earth's climate, detecting the SATAL and respective relationships with the SAMS is an important step to properly evaluate understudied potential forcings of climate change. Furthermore, the SATAL can be an important source of aerosols that can be transported to remote or pristine atmospheric regions (Gordon et al. 2017) with unknown climatic impacts.

Data and methodology

Studied area. Our study area is the Amazon basin (Fig. 1), an area that covers around 60% of the Brazilian territory and the rest in other countries (Bolivia, Peru, Ecuador, Colombia, Venezuela, Guyana, Suriname, and French Guiana). The Brazilian Amazon (so-called the legal Amazon) covers the northwest part of Brazil, where the average annual rainfall is between 1400 and 3000 mm (Cavalcante et al. 2020). Precipitation in the northern portion of the Amazon is influenced by the intertropical convergence zone (ITCZ), which moves to the Southern Hemisphere (between 4° and 10°S) during the months of March and April (Xavier et al. 2000; de Souza et al. 2004).

The rest of the basin Amazon region has a rainfall system with two well-defined seasons, with dry winters and rainy summers. In general, the region under the influence of this rainfall regime is under the influence of a monsoon regime. The SA monsoon is characterized by intense precipitation that begins, in general, in the spring and extends until March (from October to March), with its most active phase in the months of December–February, covering a large portion of the continent (Gan et al. 2004).

There are many types of aerosols found in the Amazon basin. The primary aerosols found in the Amazon region are pollen, fungal, spores, bacteria, and fragments of animals and plants (Andreae et al. 1990; Artaxo et al. 1990). The secondary organic aerosols found in the

Amazon region are new particles forming from reactions of ozone and hydroxyl with biogenic volatile organic compounds, such as isoprene and terpenes (Martin et al. 2010; Boucher 2013).

Besides that, aerosols transported from other regions also influence the Amazon basin region, mainly during the wet season, when fire over the region is almost impossible because of the high precipitation (Artaxo et al. 1990, 1993; Holanda et al. 2023), for example, the transport of biomass burning and desert dust from Africa and sea salt from the Atlantic Ocean (Artaxo et al. 2022). According to Holanda et al. (2020), during the biomass burning–influenced season (July–December), the transatlantic migration of African biomass burning smoke layers has a significant impact on the northern and central Amazonian aerosol population. From January to April, this transport travels from North Africa (north of the equator) to the Amazon region, whereas from August to November, it travels from South Africa (south of the equator) (Wang et al. 2016; Adebiyi and Zuidema 2016; Moran-Zuloaga et al. 2018; Pöhlker et al. 2018; Holanda et al. 2020).

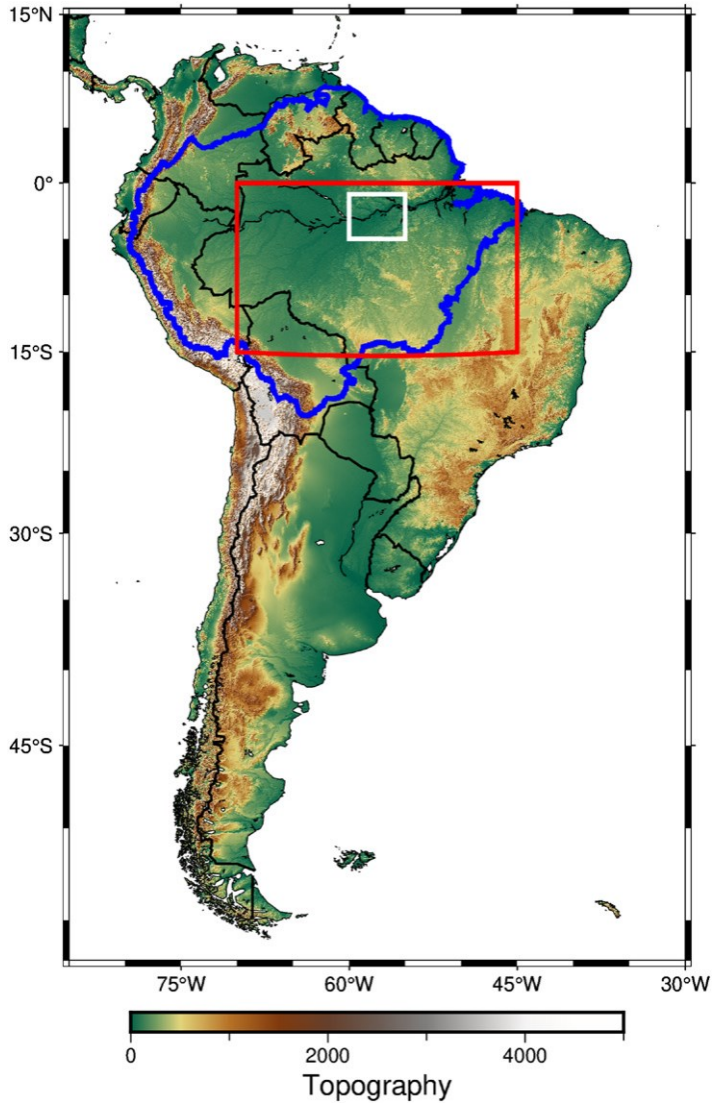

Fig. 1. South America representation and the Amazon Forest delimited by a blue line. The color bar represents the topography of the continent. The red box (0°–15°S, 45°–70°W) is the area where the SATAL is analyzed, and the white box (1°–5°S, 55°–60°W) is the area where the AE532 is maximum.

Aerosol reanalysis and satellite data. Aerosol reanalysis data used in this study are from Modern-Era Retrospective Analysis for Research and Applications (MERRA-2), produced by the Global Modeling and Assimilation Ofice at NASA's Goddard Space Flight Center. MERRA-2 is an aerosol reanalysis with 0.5° × 0.625° of spatial resolution in latitude and longitude, respectively, and 3-hourly temporal resolution. Data are available at 72 vertical levels from the surface until 0.01 hPa, generated from an assimilated system of version 5.12.4 of Goddard Earth Observing System (GEOS-5) (Gelaro et al. 2017).

MERRA-2 is an evolution of the first version of MERRA (Rienecker et al. 2011) and includes improvements related to data assimilation, newly observed data, and the assimilation of interactive aerosols. MERRA-2 is the first global reanalysis to assimilate spatial observations of aerosols and represent interactions between aerosols and other physical processes (Gelaro et al. 2017).

The aerosol variable used here was Aerosol Extinction 532 nm (AE532) from January 2002 to December 2021 from MERRA-2, although the reanalysis data were validated using

the attenuated backscatter 532 nm from CALIOP level 1.5 standard data product version V1.00. These observations have been cloud cleared and the resolution is 20 km and 60 m, horizontally and vertically, respectively, and up to 20.2 km of altitude (NASA 2019). CALIOP observations include contributions from aerosols and gas molecules (Rayleigh scattering), so the validation is limited to the total attenuated backscatter coefficient. It was computed from MERRA-2 (Randles et al. 2017; Buchard et al. 2017) only over a small period for the validation of the study.

CALIOP is one of the instruments in the *Cloud–Aerosol Lidar and Infrared Pathfinder Satellite Observations* (*CALIPSO*) satellite, which was developed by NASA's Earth System Science Pathfinder (ESSP) Program and Centre National d'Études Spatiales (CNES) (Winker et al. 2003). The *CALIPSO* mission started in 2006 with the aim of studying clouds and aerosols in the troposphere and stratosphere. *CALIPSO* flies at 705 km in polar orbit and provides measurements twice daily [0130 local time (LT) and 1330 LT] with repeated cycles of 16 days. Measurements are made using the CALIOP lidar instrument with a vertical resolution of 60 m in the upper troposphere (below 20 km) and 180 m in the stratosphere (Winker et al. 2009; Hostetler 2006).

Although most studies about a tropopause aerosol layer have used some products from the *CALIPSO* satellite data (CALIOP instrument) level 3 to identify the aerosol layer, for the tropical South America region the *CALIPSO* data level 3 are unavailable. The presence of the South Atlantic anomaly (SAA) causes dark noise in the measurements from CALIOP (Hunt et al. 2009; Noel et al. 2014; Kar et al. 2019), which could compromise the analysis. The SAA is a region located approximately within 0°–50°S, 20°E–80°W, where the Van Allen belts come down to their lowest altitude (<200 km), which expose the satellite sensors to high fluxes of energetic charged particles that are trapped within the belts (Hunt et al. 2009; Noel et al. 2014).

According to Kar et al. (2019), the primary input files used to generate level 3 are the lidar level 1B file, with the corresponding level 2.5 km merged layer and polar stratospheric clouds (PSC) mask files (Pitts et al. 2009) used for filtering. So, all data of attenuated backscatter values from *CALIPSO* L3 below the tropopause over the SAA region were removed.

Results

First, we evaluate the vertical structure of the 532 nm total attenuated backscatter of MERRA-2 sampled along the CALIOP track (level 1) during November–January 2010/11 (the validation months were chosen according to the maximum AE352 values found at UT/LS, which will be discussed below), around 0°–10°S, 50°–60°W, to validate MERRA-2. Figure 2 shows that MERRA-2 tends to exhibit a similar vertical structure as CALIOP over the Amazon basin, with maximum values of attenuated backscatter at approximately the same height.

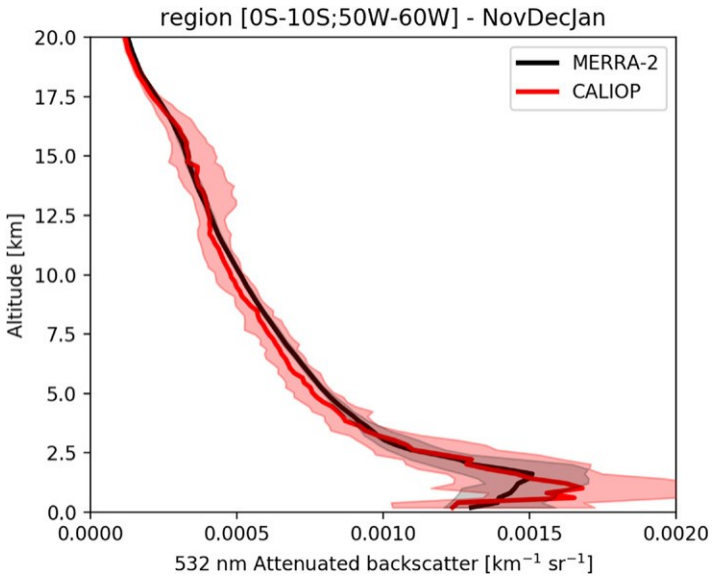

Fig. 2. Vertical profiles of total attenuated backscatter measured by CALIOP and MERRA-2 during November–January 2010/11 over the Amazon basin region, around 0°–10°S, 50°–60°W. The solid lines are the median of all CALIOP (red) and MERRA-2 (black) profiles. The shaded areas represent the 25th–75th percentiles of all modeled and observed profiles. Adapted from Buchard et al. (2016, 2017) by Virginie Buchard.

The monthly averages of MERRA-2 and CALIOP are very similar (see Figs. A1 and A2 for each month in the appendix). For example, during November, it is possible to see a little peak of attenuated backscatter above 15 km. Furthermore, although the comparison between modeled and observed data are for a short period, reanalysis data reproduce well the vertical structure of the attenuated backscatter compared to observation. It is important to point out that the 2010/11 monsoon period was chosen for this analysis because it is one of the most active periods in terms of aerosols, as will be shown below.

The mean monthly vertical distribution of AE532 from 600 to 30 hPa over the 2002–21 period is shown in Fig. 3 (see Fig. A6, from 1,000 hPa). The vertical profiles of AE532 represent a decay of aerosol concentration as pressure decreases. The curves show values higher during the monsoon period (October–March) when compared to other months. Another important point to be highlighted is the similar values around 450–130 hPa, showing the aerosol increase in this region, and the most striking result is the increase in aerosol amount above 200 hPa. These results suggest the transport of aerosols from lower levels of the atmosphere to upper levels with a spike between 130 and 200 hPa. Since this increase at upper levels occurs during the pre–rainy season (September–October) and the beginning of the SAMS rainy season (November–December and slightly in January), convective clouds could be responsible for this transport. However, the maximum convection over the Amazon during the rainy season lasts until February–March, probably the aerosols in the UT/LS should have some relation with the dry season.

Figure 4 shows monthly averages of AE532 from 2002 to 2021 in the tropopause layer (between 138 and 200 hPa, about 11–14 km height) from MERRA-2, and Fig. 5 shows its vertical evolution. The SATAL is clearly visible in Fig. 4 over the Amazon basin, with maximum values in October and November (red color), consistent with Fig. 3. The SATAL begins to form in September (Figs. 3–5), but it did not fully develop until October, with its peak values in the eastern Amazon basin (around 5°S, 55°W). Then the SATAL is extended westward to the southern Amazon (around 10°S, 60°W) during November, when it is most intense and reaches the highest altitude. It weakens in December and January and finally dissipates in February–March. It is almost nonexistent during other months. The aerosol extinction

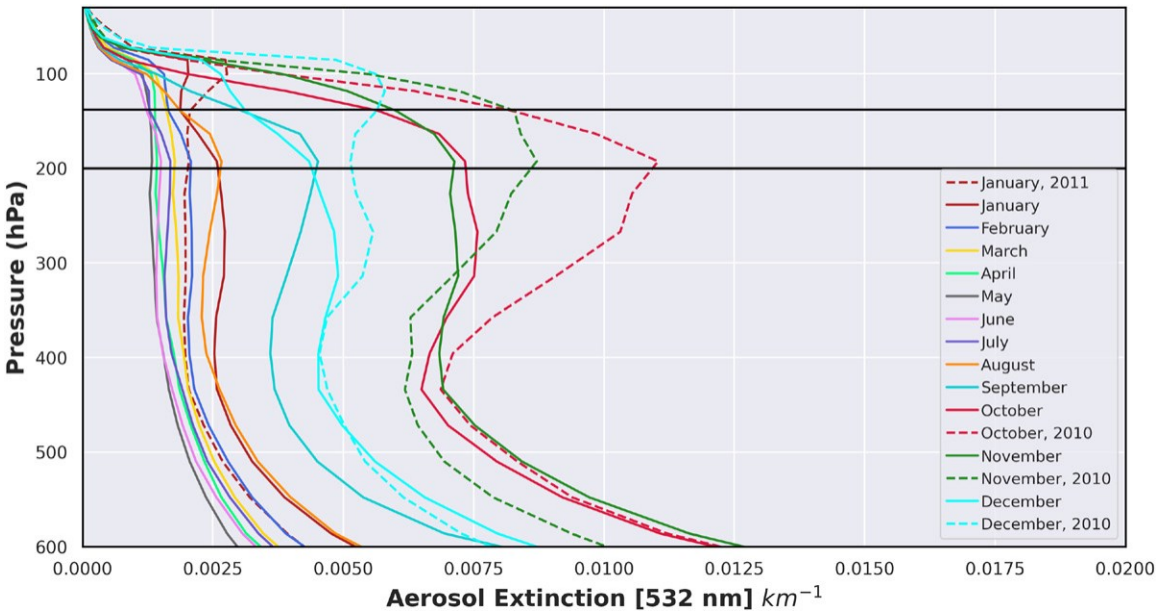

Fig. 3. Mean monthly vertical distribution of the aerosol extinction 532 nm from MERRA-2 over the white box shown in Fig. 1. The solid color lines represent the mean of each month, the dashed color lines represent the peak months, and the two black horizontal lines show the altitude where the AE532 is maximum over the upper troposphere.

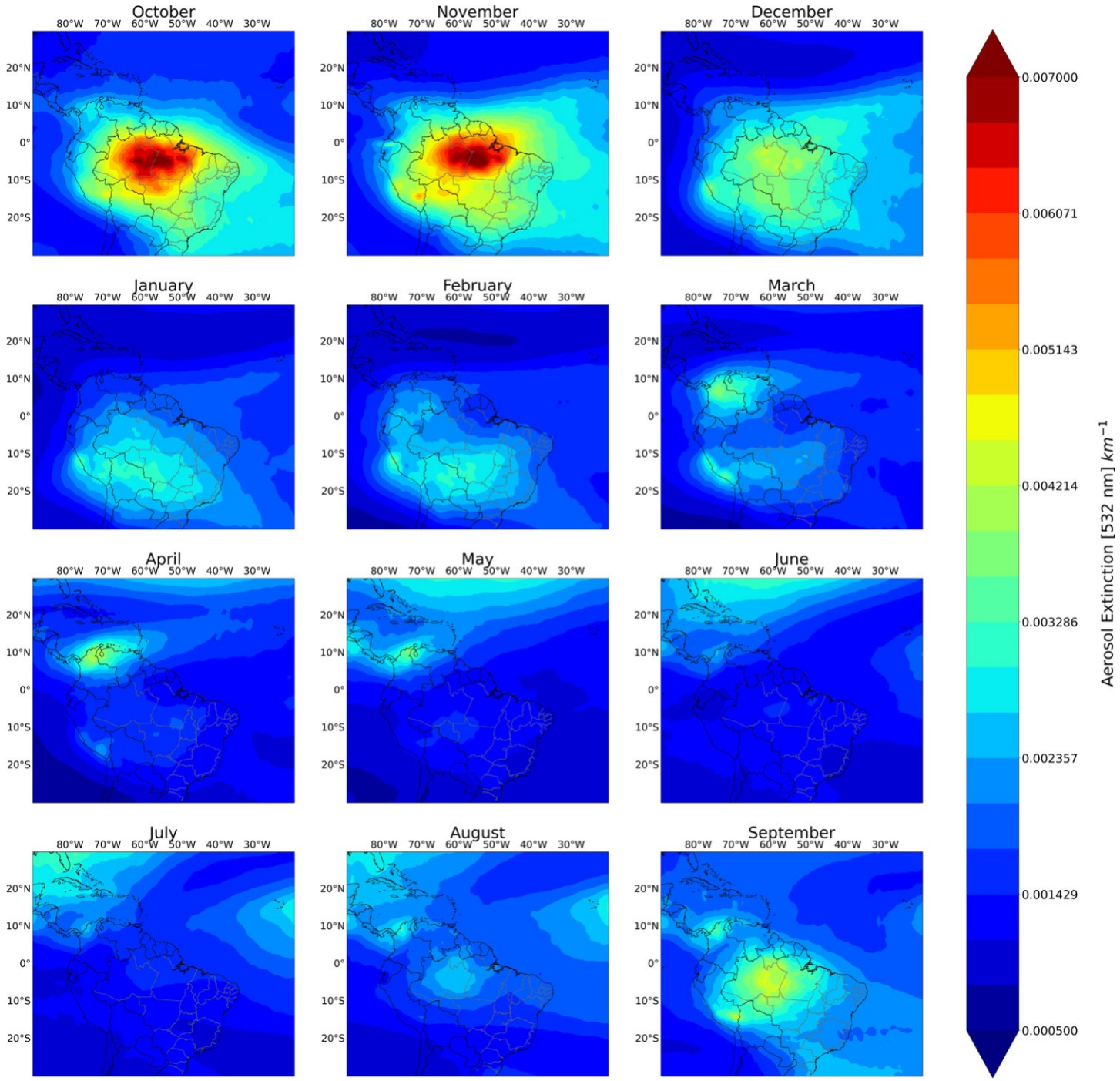

Fig. 4. Maps of the monthly mean of the aerosol extinction from MERRA-2 between 138 and 220 hPa during 2002–21.

reaches its maximum altitude (about 85 hPa, 17 km) during January (Figs. 3 and 5), although during January it is much weaker than previous months, probably due to the scavenging of aerosol particles by intense precipitation.

SATAL exhibits significant interannual variability, as the mean of AE532 time series within a box roughly bounding the Amazon region indicates (about 0°–15°S, 45°–70°W; see the red box in Fig. 1) (Fig. 6). The maximum AE532 is in phase between 11 and 14 km during all the periods. The maximum AE532 varies over the years, but most occur within 11 km during October and November. Although the average value of AE532 is around 0.006 km^{-1} (Fig. 6), there are some extreme values, for example, during the summer between 2010 and 2011. For instance, minimum values during the weak El Niño event of 2005/06 (due to weak

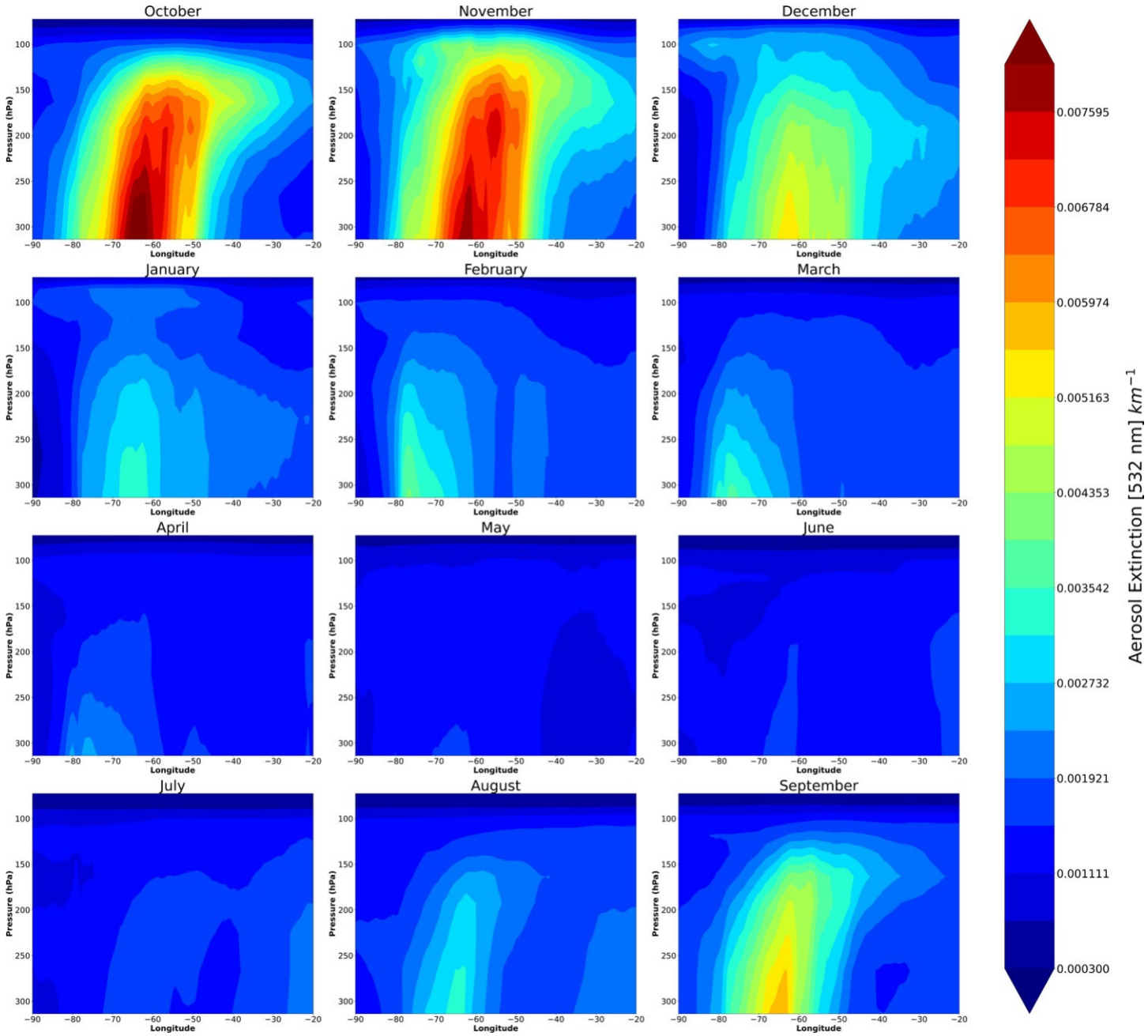

Fig. 5. Mean monthly longitudinal cross section of aerosol extinction in 1°–5°S, over the white box shown in Fig. 1. The *y*-axis plot is between 313 and 72 hPa.

convective activity over the Amazon basin) and maximum values during the strong La Niña event of 2010/11 (due to intense convection over the Amazon basin).

Discussion and conclusions

The comparison between vertical profiles of the 532 nm total attenuated backscatter from MERRA-2 and CALIOP data over the Amazon region (at 0°–10°S, 50°–60°W) shows great agreement. This result gives confidence to use MERRA-2 data to study aerosols in the UT/LS and the presence of the SATAL over the Amazon basin. Results from MERRA-2 clearly show the presence of the SATAL over South America, specifically over the Amazon basin, with maximum values between October and November (Fig. 3). SATAL forms first in the eastern Amazon basin, then moves westward to the southern Amazon, where it weakens in December–January

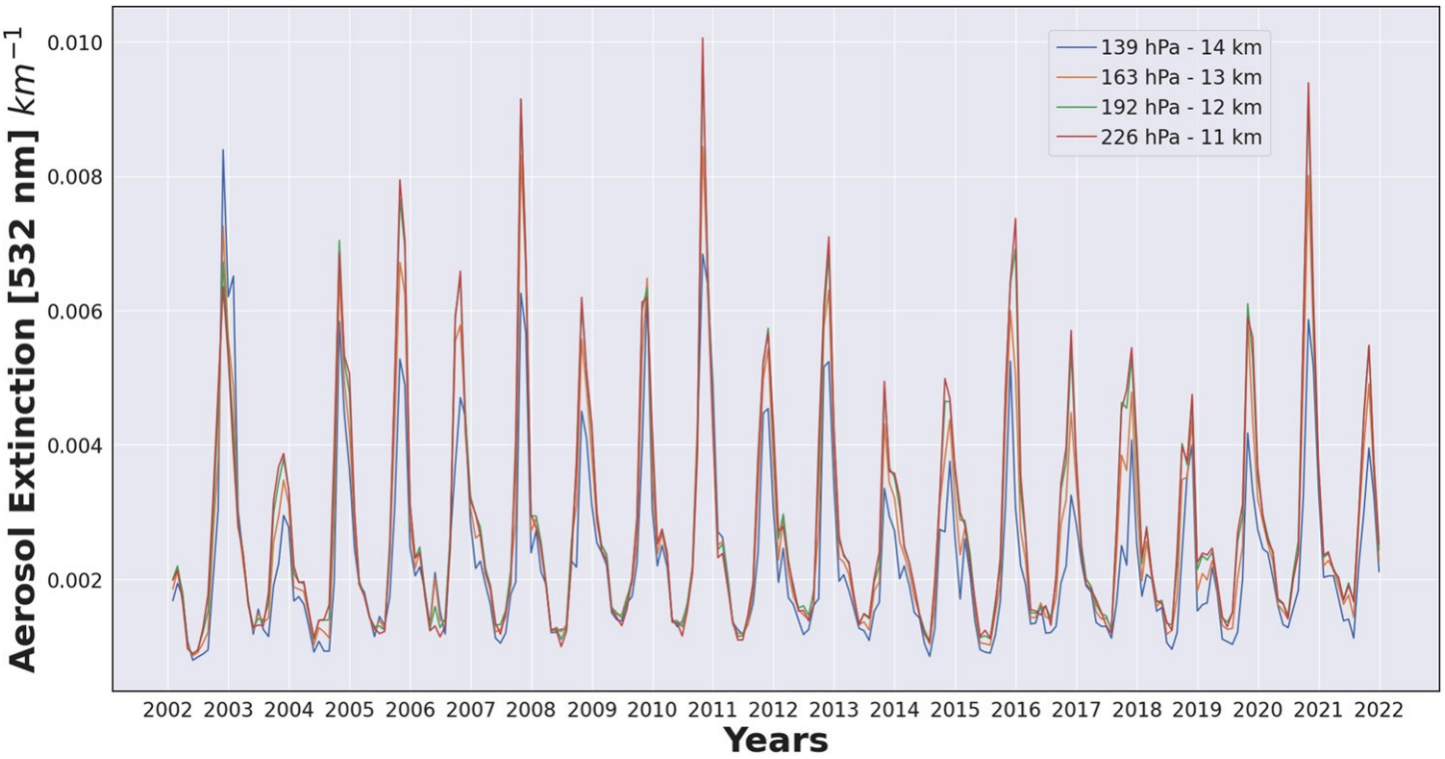

Fig. 6. Time series of the mean MERRA-2 aerosol extinction from 2002 to 2021 at 139 hPa (blue line), 163 hPa (orange line), 192 hPa (green line), and 226 hPa (red line) over the red box area shown in Fig. 1 (0°–15°S, 45°–70°W).

and finally dissipates in February–March. This is consistent with the vertical SATAL structure (Fig. 4), which shows a similar life cycle as in Fig. 3. The annual mean AE532 at around 226, 192, 163, and 139 hPa (approximately 11, 12, 13, and 14 km, respectively; Fig. 6) suggests that extreme values of AE532 are related to changes in convective activity due to ENSO events, minimum values during the El Niño event of 2005/06 (weak convective activity over the Amazon basin) and maximum values during the La Niña event of 2011/12 (intense convection over the Amazon basin). Furthermore, it is still possible that there may be a relationship between the seasonality of SATAL and the ENSO oscillation (see Fig. A7), but this will be investigated in the future. The lowest values of AE532 during some periods of intense drought over southeastern Brazil, as in 2014, suggest some linkages between SATAL and SAMS. Intriguingly, SATAL is only present between October and March, during the South American wet season and the active period of SAMS (with Amazon convection and SACZ well established).

The existence of aerosols at around 11–14 km altitude obtained from MERRA-2 is consistent with the existence of nanoparticles in the upper troposphere between 8 and 15 km altitude identified during the GoAmazon2014/5 campaign (Martin et al. 2016; Andreae et al. 2018). This present study shows the existence of the SATAL at around 11–14 km height over the Amazon basin with seasonal behavior similar to the ATAL and NATAL (Vernier et al. 2011; Thomason and Vernier 2013), confirming the presence of the SATAL over South America.

Our results suggest two main factors related to SATAL formation and dissipation. The aerosol source in the Amazon basin's lower troposphere may originate from Africa, which agrees with the lower-troposphere circulation pattern (see Fig. A4) and previous studies (Pöhlker et al. 2018; Pöhlker et al. 2019; Holanda et al. 2020). In addition, aerosol concentrations increase throughout the atmosphere at the beginning of the rainy season (October, Fig. 3), suggesting that aerosols released by the Amazon rain forest during the dry season may be

another aerosol source (see monthly precipitation average in Fig. A5). On the other hand, the fact that SATAL develops during October–November suggests that the second factor for SATAL formation is associated with intense convection over the Amazon basin (see Fig. A3). The updraft mass flux of the deep convective systems must be responsible for the vertical transport from the lower atmosphere to the upper troposphere/lower stratosphere. These hypotheses are being analyzed for a new article that is under development.

Previous studies have already shown that convection is efficient in transporting particles or trace gases from the lower troposphere to the upper troposphere. Based on measurements carried out in the Amazon during the ACRIDICON–CHUVA 2014 campaign, Andreae et al. (2018) showed high aerosol particle concentrations in the UT between 8 and 15 km altitude, with a number higher than those in the planetary boundary layer (PBL), and suggest that the aerosol distribution structure is directly related to deep convection. Furthermore, these aerosols would be a source of CCN for the PBL, through convective downdrafts (Andreae et al. 2018; Wang et al. 2016). Machado et al. (2021) combined in situ measurements of aerosol and remote sensing data to evaluate the effect of weather events on the particle size distribution at the Amazon Tall Tower Observatory (ATTO). The authors showed that the ultrafine particles concentration changes with the convective rain, which indicates a relationship between vertical transport and deep convective clouds.

In conclusion, we identified the existence of the SATAL over the Amazon basin at around 11–14 km height, with maximum values between October and November, which shows that there is a relationship between vertical transport and deep convective clouds. Nevertheless, questions about its origin and relation with SAMS, ENSO, droughts, and its influence on remote regions through high levels are open. Furthermore, the relationship between SATAL and SAMS must be clarified. It is necessary to use observational and modeling studies to answer these questions.

During December 2022 and January 2023, the field experiment called Chemistry of the Atmosphere: Field Experiment in Brazil (CAFE-Brazil) took place over the Amazon region (Herdies et al. 2021). The experiment used the High-Altitude Long-Range (HALO) aircraft to make chemistry and aerosol measurements in the upper troposphere. It is expected that the observations that were collected during the CAFE-Brazil experiment can provide useful information to confirm the existence of SATAL and to find the origin and composition of the aerosols in the UT/LS during the South American monsoon.

Acknowledgments. This study is part of the graduate program in Meteorology at the National Institute for Space Research (INPE). This study was financed in part by the Coordination for the Improvement of Higher Education Personnel–Brazil (CAPES-Brazil), Finance Code 001, and it was partially developed during the CAPES-PrInt Project (88887.696391/2022-00). The authors thank CAPES (88881.148662/2017-01) for their support and INPE for the availability of their infrastructure. The authors are also grateful to the University of California, Santa Barbara, for their infrastructure during the CAPES-PrInt project. We also thank the National Council for Scientific and Technological Development (CNPq, Brazil). The authors would also like to thank Ravi C. Govindaraju for his help in making the MERRA-2 data available. C. Jones and L. M. V. Carvalho would like to thank the finan-cial support from the National Science Foundation (AGS 1937899). We would like to acknowledge high-performance computing support from Cheyenne (doi: 10.5065/D6RX99HX) provided by NCAR's Computational and Information Systems Laboratory, sponsored by the National Science Foundation.

Data availability statement. The MERRA-2 data have been downloaded using Earthdata available at https://disc.gsfc.nasa.gov and https://giovanni.gsfc.nasa.gov/giovanni/. The *CALIPSO* satellite data were obtained by Virginie Buchard from https://www-calipso.larc.nasa.gov.

Appendix: Figures to complement the discussions of the results

This appendix contains Figs. A1–A7. Figures A1 and A2 present the vertical profiles of total attenuated backscatter measured by CALIOP and MERRA-2 over the Amazon basin region, around 0°–10°S, 50°–65°W during November 2010 and December 2010, respectively, for CALIOP and MERRA-2 profiles. The monthly height–longitude cross section of vertical velocity (Pa s^{-1}) over 0°–15°S from MERRA-2 data from 2002 to 2021 is shown in Fig. A3. Figure A4 shows the composite of the speed (shaded) and direction (vectors) 850 hPa wind from 2002 to 2021 averaged over South America from MERRA-2 data. Figure A5 shows the monthly precipitation average (mm day^{-1}) from 2002 to 2021 from MERRA-2 data over South America. Figure A6 shows the mean monthly vertical distribution of the aerosol extinction 532 nm from MERRA-2 in the area 1°–5°S, 55°–60°W, the same as in Fig. 3, but now the *y*-axis plot is from 1,000 hPa. Figure A7 shows the South America representation, with the Amazon Forest indicated by the blue line. The red box (area 1) represents the area 12°S–2°N, 80°–70°W; the yellow box (area 2) represents the area 5°S–8°N, 70°–55°W; the orange box (area 3) represents the area 19°–5°S, 70°–55°W; and the purple box (area 4) represents the area 15°S–3°N, 55°–48°W. Time series of the mean MERRA-2 aerosol extinction (AE532) from 2002 to 2021 are shown at 139, 163, 192, and 226 hPa, with the representation of two strong La Niña periods (blue band) and a strong El Niño period (red band).

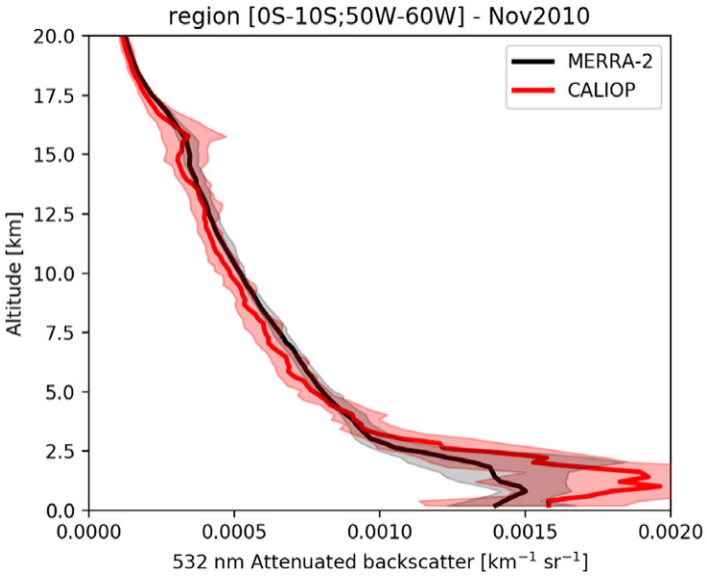

Fig. A1. Vertical profiles of total attenuated backscatter measured by CALIOP and MERRA-2 during November 2010 over the Amazon basin region, around 0°–10°S, 50°–65°W. The solid lines are the median of all CALIOP (red) and MERRA-2 (black) profiles. The shaded areas represent the 25th–75th percentiles of all modeled and observed profiles. Adapted from Buchard et al. (2016, 2017) by Virginie Buchard.

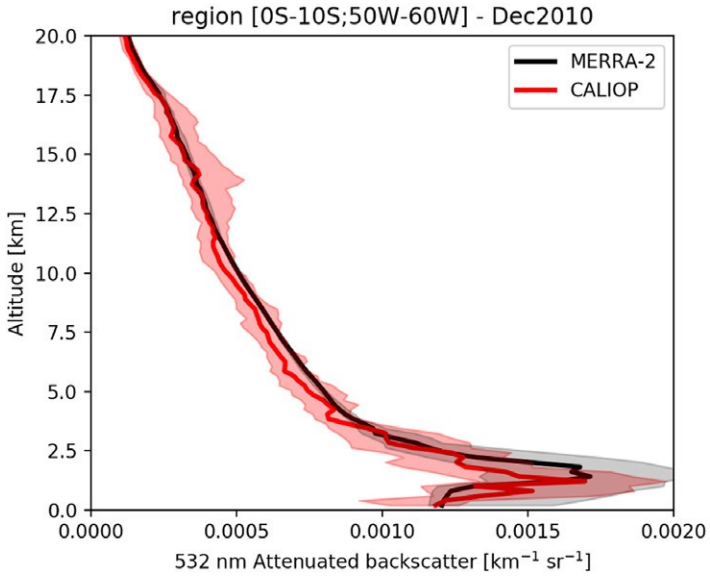

Fig. A2. Vertical profiles of total attenuated backscatter measured by CALIOP and MERRA-2 during December 2010 over the Amazon basin region, around 0°–10°S, 50°–65°W. The solid lines are the median of all CALIOP (red) and MERRA-2 (black) profiles. The shaded areas represent the 25th–75th percentiles of all modeled and observed profiles. Adapted from Buchard et al. (2016, 2017) by Virginie Buchard.

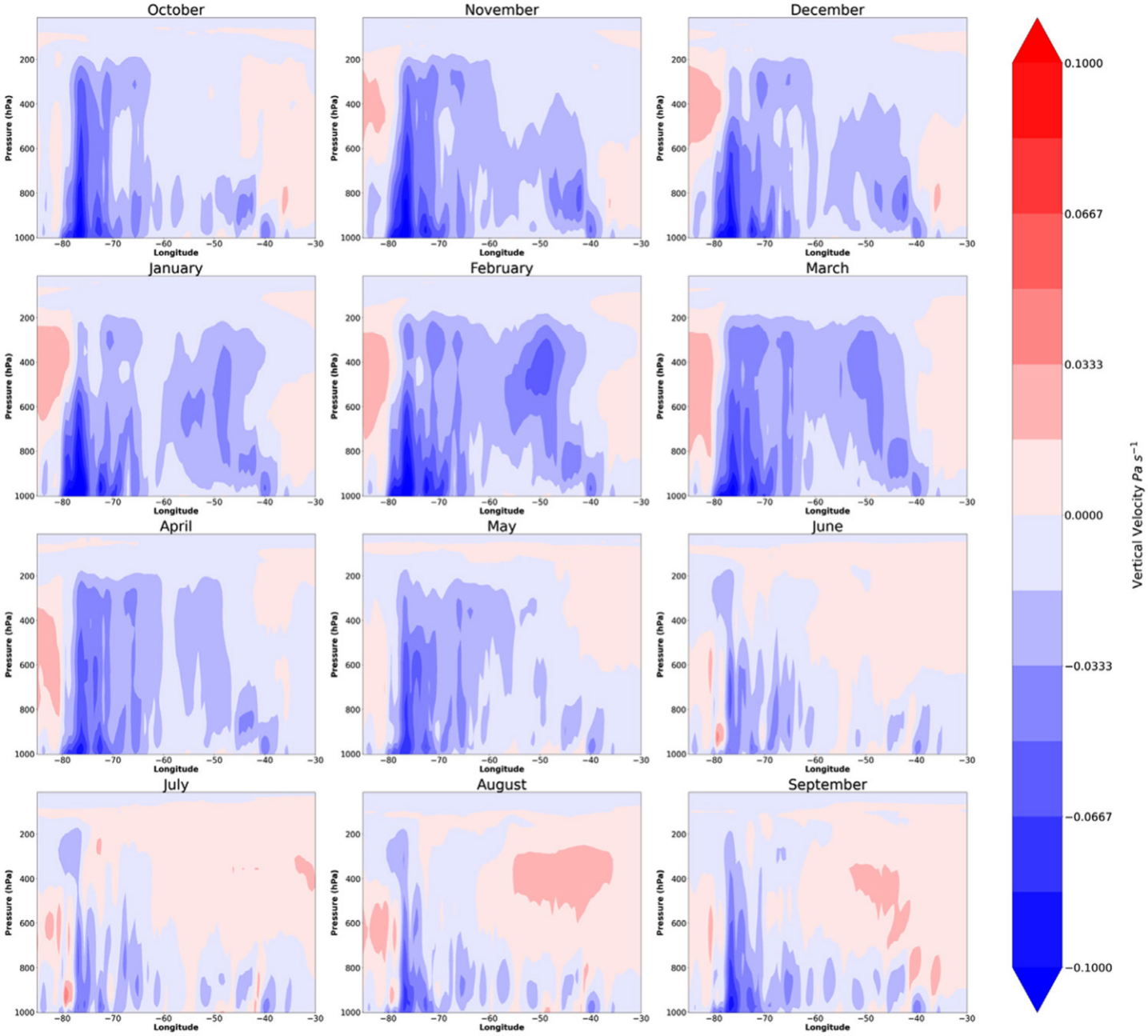

Fig. A3. Monthly height–longitude cross section of vertical velocity (Pa s^{-1}) over 0°–15°S from MERRA-2 data from 2002 to 2021. Upward motion (downward motion) denoted with negative (positive) values.

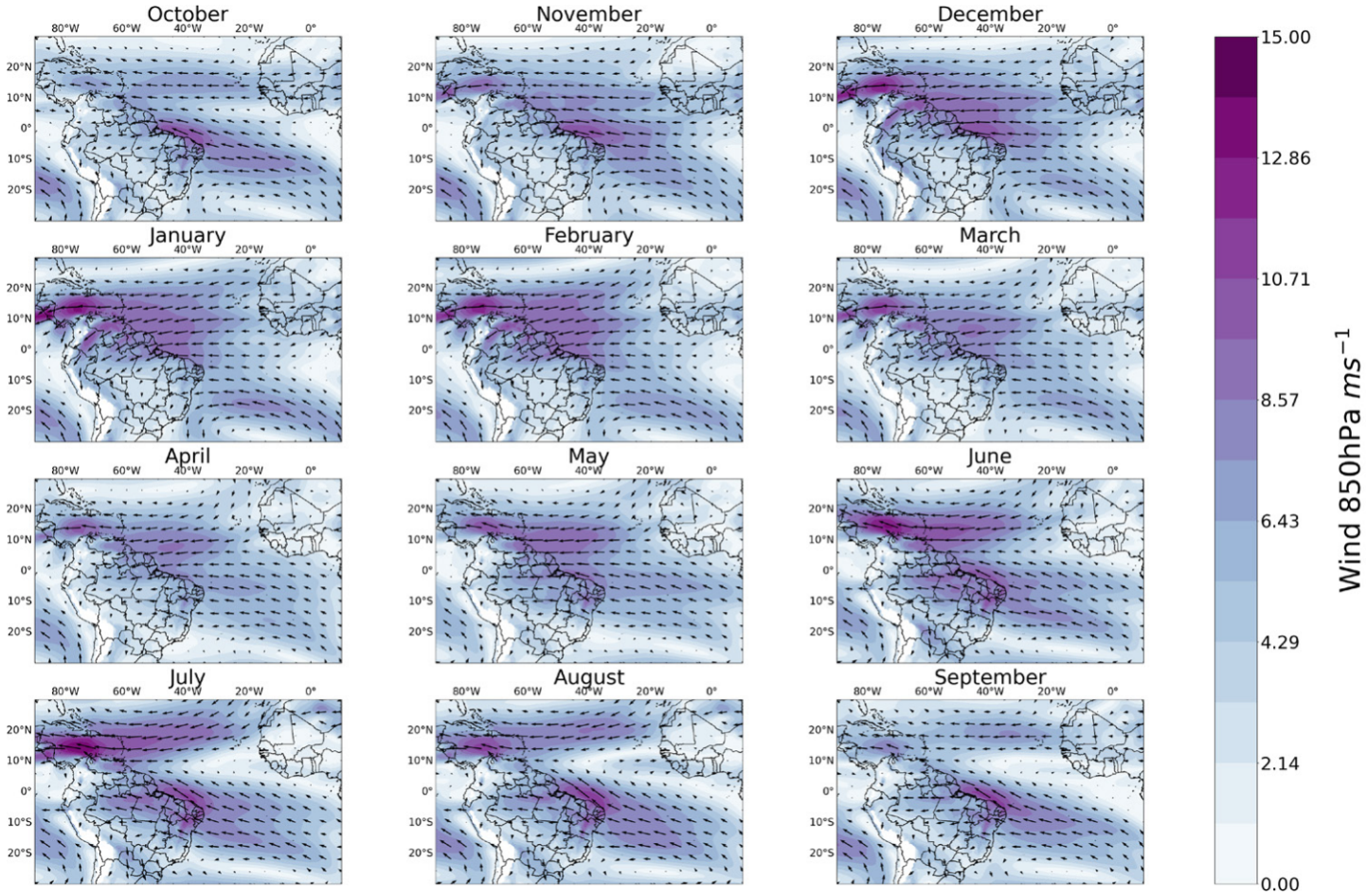

Fig. A4. Composite of the speed (shaded) and direction (vectors) 850 hPa wind from 2002 to 2021 averaged over South America from MERRA-2 data.

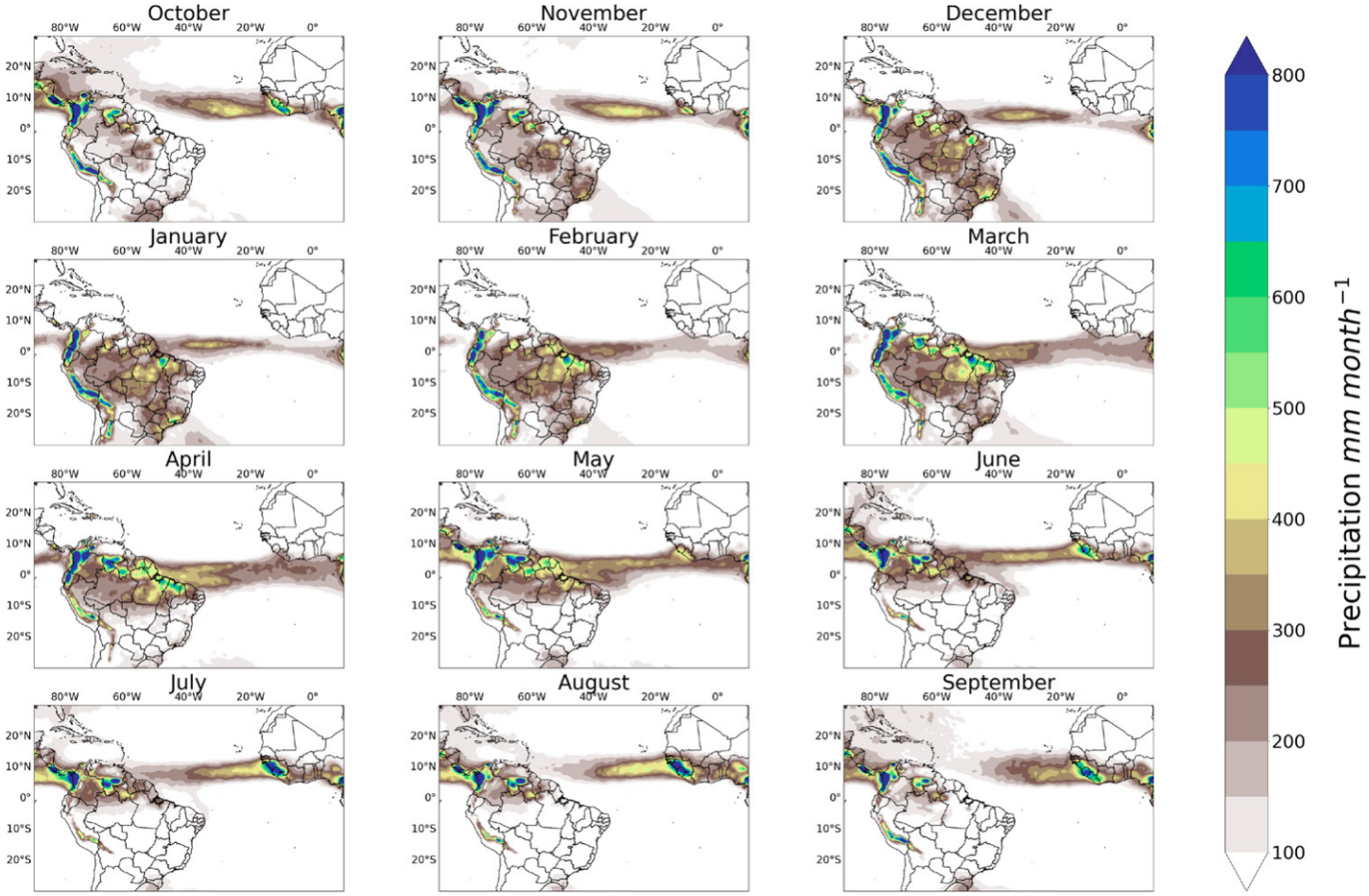

Fig. A5. Monthly precipitation averaged (mm day^{-1}) from 2002 to 2021 from MERRA-2 data over South America.

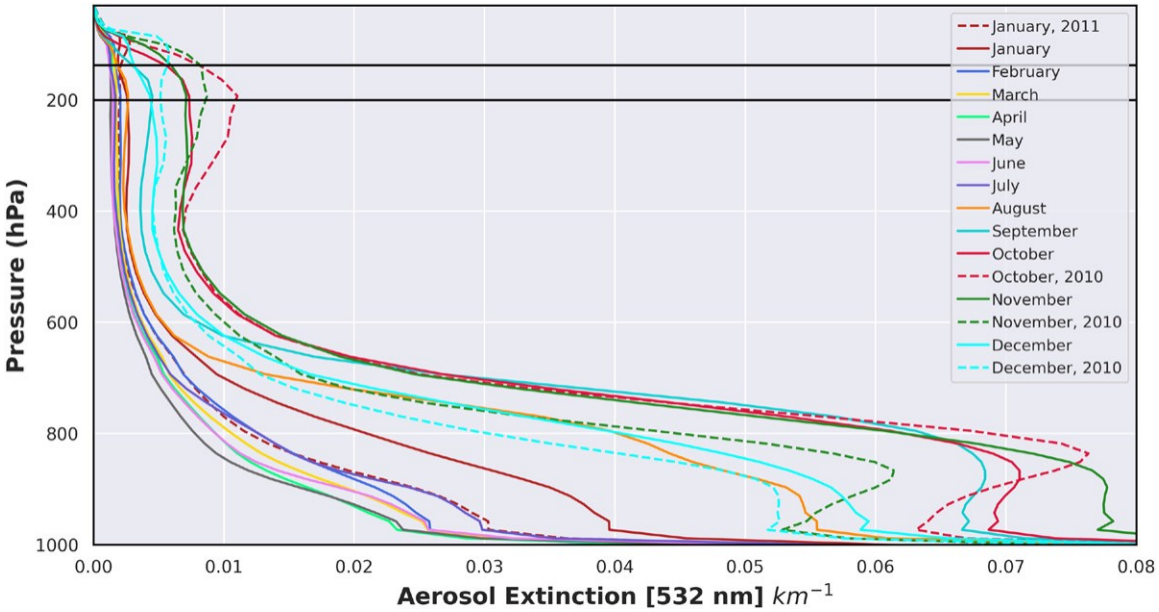

Fig. A6. Mean monthly vertical distribution of the aerosol extinction 532 nm from MERRA-2 in the area 1°–5°S, 55°–60°W. The *y*-axis plot is from 1,000 hPa.

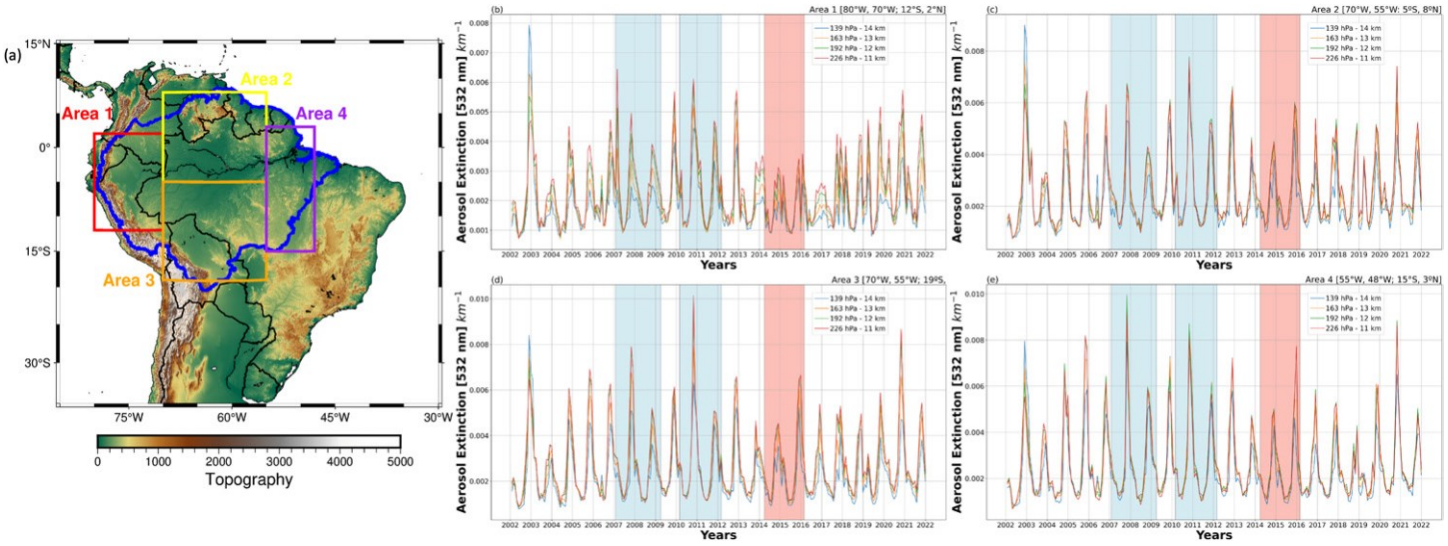

Fig. A7. (a) South America representation and the Amazon Forest shown by the blue line. The color bar represents the topogra-phy of the continent. The red box (area 1) represents the area 12°S–2°N, 80°–70°W; the yellow box (area 2) represents the area 5°S–8°N, 70°–55°W; the orange box (area 3) represents the area 19°–5°S, 70°–55°W; and the purple box (area 4) represents the area 15°S–3°N, 55°–48°W. (b) Time series of the mean MERRA-2 aerosol extinction (AE532) from 2002 to 2021 at 139 hPa (blue line), 163 hPa (orange line), 192 hPa (green line), and 226 hPa (red line) over the red box area. (c) As in (b), but over the yellow box. (d) As in (b), but over the orange box. (e) As in (b), but over the purple box. In (b)–(e), the blue band represents two strong La Niña periods and the red band represents a strong El Niño period.

References

Adebiyi, A. A. and P. Zuidema, 2016: The role of the southern African easterly jet in modifying the southeast Atlantic aerosol and cloud environments. Quart. J. Roy. Meteor. Soc., **142**, 1574–1589, https://doi.org/10.1002/qj.2765.

Andreae, M. O., H. Berresheim, H. Bingemer, D. J. Jacob, B. L. Lewis, S. M. Li, and R. W. Talbot, 1990: The atmospheric sulfur cycle over the Amazon basin: 2. Wet season. J. Geophys. Res., **95**, 16 813–16 824, https://doi.org/10.1029/JD095iD10p16813.

——, and Coauthors, 2018: Aerosol characteristics and particle production in the upper troposphere over the Amazon basin. Atmos. Chem. Phys., **18**, 921–961, https://doi.org/10.5194/acp-18-921-2018.

Artaxo, P., W. Maenhaut, H. Stroms, and R. Van Grieken, 1990: Aerosol characteristics and sources for the Amazon basin during the wet season. J. Geophys. Res., **951**, 16 971–16 985, https://doi.org/10.1029/JD095iD10p16971.

——, M. Yamasoe, J. Martins, S. Kocinas, S. Car-Vallo, and W. Maenhaut, 1993: Case study of atmospheric measurements in Brazil: Aerosol emissions from Amazon basin fires. Fire in the Environment: The Ecological, Atmospheric, and Climatic Importance of Vegetation Fires, P. J. Crutzen and J. G. Goldammer, Eds., Environmental Sciences Research Rep. 13, Wiley, 139–158.

——, and Coauthors, 2022: Tropical and boreal forest atmosphere interactions: A review. Tellus, **74B**, 24–163, https://doi.org/10.16993/tellusb.34.

Boucher, O., 2013: Atmospheric Aerosols: Properties and Climate Impacts. Springer, 311 pp.

Buchard, V., and Coauthors, 2016: Evaluation of the surface PM2.5 in version 1 of the NASA MERRA aerosol reanalysis over the United States. Atmos. Environ., **125**, 100–111, https://doi.org/10.1016/j.atmosenv.2015.11.004.

——, and Coauthors, 2017: The MERRA-2 aerosol reanalysis, 1980 onward. Part II: Evaluation and case studies. J. Climate, **30**, 6851–6872, https://doi.org/10.1175/JCLI-D-16-0613.1.

Carvalho, L. M. V., C. Jones, and B. Liebmann, 2004: The South Atlantic convergence zone: Intensity, form, persistence, and relationships with intraseasonal to interannual activity and extreme rainfall. J. Climate, **17**, 88–108, https://doi.org/10.1175/1520-0442(2004)017<0088:TSACZI>2.0.CO;2.

Cavalcante, R., D. Ferreira, P. Pontes, R. Tedeschi, C. Wanzeler da Costa, and E. De Souza, 2020: Evaluation of extreme rainfall indices from CHIRPS precipitation estimates over the Brazilian Amazonia. Atmos. Res., **238**, 104879, https://doi.org/10.1016/j.atmosres.2020.104879.

Coelho, C. A., and Coauthors, 2022: Assessing the representation of South American monsoon features in Brazil and UK climate model simulations. Climate Resilience Sustainability, **1**, e27, https://doi.org/10.1002/cli2.27.

da Silva, A. E., and L. M. V. de Carvalho, 2007: Large-scale index for South America monsoon (LISAM). Atmos. Sci. Lett., **8**, 51–57, https://doi.org/10.1002/asl.150.

de Souza, E. B., M. T. Kayano, and T. Ambrizzi, 2004: The regional precipitation over the eastern Amazon/Northeast Brazil modulated by tropical Pacific and Atlantic SST anomalies on weekly timescale. Rev. Bras. Meteor., **19**, 113–122.

Gan, M. A., V. E. Kousky, and C. F. Ropelewski, 2004: The South America monsoon circulation and its relationship to rainfall over west-central Brazil. J. Climate, **17**, 47–66, https://doi.org/10.1175/1520-0442(2004)017<0047:TSAMCA>2.0.CO;2.

Gelaro, R., and Coauthors, 2017: The Modern-Era Retrospective Analysis for Research and Applications, version 2 (MERRA-2). J. Climate, **30**, 5419–5454, https://doi.org/10.1175/JCLI-D-16-0758.1.

Gordon, H., and Coauthors, 2017: Causes and importance of new particle formation in the present-day and preindustrial atmospheres. J. Geophys. Res. Atmos., **122**, 8739–8760, https://doi.org/10.1002/2017JD026844.

Herdies, D. L., V. E. Kousky, and W. Ebisuzaki, 2007: The impact of high-resolution SALLJEX data on global NCEP analyses. J. Climate, **20**, 5765–5783, https://doi.org/10.1175/2007JCLI1375.1.

——, J. Lelieveld, L. A. T. Machado, U. Pöschl, P. Artaxo, and J. Curtius, 2021: Quíimica da atmosfera: Experimento de campo no Brasil – CAFE-Brazil (Chemistry of the atmosphere: Field experiment in Brazil – CAFE-Brazil). Tech. Rep., 40 pp., https://www.researchgate.net/publication/377148642_Quiimica_da_atmosfera_Experimento_de_campo_no_Brasil_-_CAFE-Brazil_Chemistry_of_the_atmosphere_Field_experiment_in_Brazil_-_CAFE-Brazil.

Holanda, B. A., and Coauthors, 2020: Influx of African biomass burning aerosol during the Amazonian dry season through layered transatlantic transport of black carbon-rich smoke. Atmos. Chem. Phys., **20**, 4757–4785, https://doi.org/10.5194/acp-20-4757-2020.

——, and Coauthors, 2023: African biomass burning affects aerosol cycling over the Amazon. Commun. Earth Environ., **4**, 154, https://doi.org/10.1038/s43247-023-00795-5.

Hostetler, C. A., and Coauthors, 2006: Calibration and level 1 data products. CALIOP Algorithm Theoretical Basis Doc. PC-SCI-201, 66 pp., https://ccplot.org/pub/resources/CALIPSO/CALIOP%20Algorithm%20Theoretical%20Basis%20Document/PC-SCI-201%20Calibration%20and%20Level%201%20Data%20Products.pdf.

Hunt, W., D. Winker, M. Vaughan, K. Powell, P. Lucker, and C. Weimer, 2009: CALIPSO lidar description and performance assessment. J. Atmos. Oceanic Technol., **26**, 1214–1228, https://doi.org/10.1175/2009JTECHA1223.1.

Kar, J., K.-P. Lee, M. A. Vaughan, J. L. Tackett, C. R. Trepte, D. M. Winker, P. L. Lucker, and B. J. Getzewich, 2019: CALIPSO level 3 stratospheric aerosol profile product: Version 1.00 algorithm description and initial assessment. Atmos. Meas. Tech., **12**, 6173–6191, https://doi.org/10.5194/amt-12-6173-2019.

Kodama, Y., 1992: Large-scale common features of subtropical precipitation zones (the Baiu frontal zone, the SPCZ, and the SACZ) Part I: Characteristics of subtropical frontal zones. J. Meteor. Soc. Japan, **70**, 813–836, https://doi.org/10.2151/jmsj1965.70.4_813.

Lau, W., C. Yuan, and Z. Li, 2018: Origin, maintenance and variability of the Asian tropopause aerosol layer (ATAL): The roles of monsoon dynamics. Sci. Rep., **8**, 3960, https://doi.org/10.1038/s41598-018-22267-z.

Machado, L. A. T., and Coauthors, 2021: How weather events modify aerosol particle size distributions in the Amazon boundary layer. Atmos. Chem. Phys., **21**, 18 065–18 086, https://doi.org/10.5194/acp-21-18065-2021.

Marengo, J. A., W. R. Soares, C. Saulo, and M. Nicolini, 2004: Climatology of the low-level jet east of the Andes as derived from the NCEP–NCAR reanalyses: Characteristics and temporal variability. J. Climate, **17**, 2261–2280, https://doi.org/10.1175/1520-0442(2004)017<2261:COTLJE>2.0.CO;2.

——, and Coauthors, 2012: Recent developments on the South American monsoon system. Int. J. Climatol., **32**, 1–21, https://doi.org/10.1002/joc.2254.

Martin, S. T., and Coauthors, 2010: An overview of the Amazonian Aerosol Characterization Experiment 2008 (AMAZE-08). Atmos. Chem. Phys., **10**, 11 415–11 438, https://doi.org/10.5194/acp-10-11415-2010.

——, and Coauthors, 2016: Introduction: Observations and modeling of the Green Ocean Amazon (GoAmazon2014/5). Atmos. Chem. Phys., **16**, 4785–4797, https://doi.org/10.5194/acp-16-4785-2016.

Merikanto, J., D. Spracklen, G. Mann, S. Pickering, and K. Carslaw, 2009: Impact of nucleation on global CCN. Atmos. Chem. Phys., **9**, 8601–8616, https://doi.org/10.5194/acp-9-8601-2009.

Montini, T. L., C. Jones, and L. M. V. Carvalho, 2019: The South American low-level jet: A new climatology, variability, and changes. J. Geophys. Res. Atmos., **124**, 1200–1218, https://doi.org/10.1029/2018JD029634.

Moran-Zuloaga, D., and Coauthors, 2018: Long-term study on coarse mode aerosols in the Amazon rain forest with the frequent intrusion of Saharan dust plumes. Atmos. Chem. Phys., **18**, 10 055–10 088, https://doi.org/10.5194/acp-18-10055-2018.

Myhre, G., and Coauthors, 2013: Anthropogenic and natural radiative forcing. Climate Change 2013: The Physical Science Basis, T. F. Stocker et al., Eds. Cambridge University Press, 661–740.

NASA, 2019: CALIPSO lidar level 1.5 profile, V1-00. NASA Langley Atmospheric Science Data Center DAAC, accessed April 2023, https://doi.org/10.5067/CALIOP/CALIPSO/LID_L15-STANDARD-V1-00.

Noel, V., H. Chepfer, C. Hoareau, M. Reverdy, and G. Cesana, 2014: Effects of solar activity on noise in CALIOP profiles above the South Atlantic anomaly. Atmos. Meas. Tech., **7**, 1597–1603, https://doi.org/10.5194/amt-7-1597-2014.

Pierce, J., and P. Adams, 2009: Uncertainty in global CCN concentrations from uncertain aerosol nucleation and primary emission rates. Atmos. Chem. Phys., **9**, 1339–1356, https://doi.org/10.5194/acp-9-1339-2009.

Pitts, M., L. Poole, and L. Thomason, 2009: CALIPSO polar stratospheric cloud observations: Second-generation detection algorithm and composition discrimination. Atmos. Chem. Phys., **9**, 7577–7589, https://doi.org/10.5194/acp-9-7577-2009.

Pöhlker, C., and Coauthors, 2019: Land cover and its transformation in the backward trajectory footprint region of the Amazon Tall Tower Observatory. Atmos. Chem. Phys., **19**, 8425–8470, https://doi.org/10.5194/acp-19-8425-2019.

Pöhlker, M. L., and Coauthors, 2018: Long-term observations of cloud condensation nuclei over the Amazon rain forest–Part 2: Variability and characteristics of biomass burning, long-range transport, and pristine rain forest aerosols. Atmos. Chem. Phys., **18**, 10 289–10 331, https://doi.org/10.5194/acp-18-10289-2018.

Randles, C., and Coauthors, 2017: The MERRA-2 aerosol reanalysis, 1980 onward. Part I: System description and data assimilation evaluation. J. Climate, **30**, 6823–6850, https://doi.org/10.1175/JCLI-D-16-0609.1.

Rienecker, M., and Coauthors, 2011: MERRA: NASA's Modern-Era Retrospective Analysis for Research and Applications. J. Climate, **24**, 3624–3648, https://doi.org/10.1175/JCLI-D-11-00015.1.

Salio, P., M. Nicolini, and A. C. Saulo, 2002: Chaco low-level jet events characterization during the austral summer season. J. Geophys. Res., **107**, 4816, https://doi.org/10.1029/2001JD001315.

Seinfeld, J. H., and S. N. Pandis, 2016: Atmospheric Chemistry and Physics: From Air Pollution to Climate Change. John Wiley and Sons, 1120 pp.

Silva, V., and V. Kousky, 2012: The South American Monsoon System: Climatology and Variability. Modern Climatology, S.-Y. Wang and R. R. Gillies, Eds., Intech-Open, 32 pp., https://doi.org/10.5772/38565.

Thomason, L., and J. Vernier, 2013: Improved SAGE II cloud/aerosol categorization and observations of the Asian tropopause aerosol layer: 1989–2005. Atmos. Chem. Phys., **13**, 4605–4616, https://doi.org/10.5194/acp-13-4605-2013.

Twomey, S., 1977: The influence of pollution on the shortwave albedo of clouds. J. Atmos. Sci., **34**, 1149–1152, https://doi.org/10.1175/1520-0469(1977)034<1149:TIOPOT>2.0.CO;2.

Vera, C., and Coauthors, 2006: Toward a unified view of the American monsoon systems. J. Climate, **19**, 4977–5000, https://doi.org/10.1175/JCLI3896.1.

Vernier, J.-P., L. W. Thomason, and J. Kar, 2011: CALIPSO detection of an Asian tropopause aerosol layer. Geophys. Res. Lett., **38**, L07804, https://doi.org/10.1029/2010GL046614.

Wang, H., and R. Fu, 2004: Influence of cross-Andes flow on the South American low-level jet. J. Climate, **17**, 1247–1262, https://doi.org/10.1175/1520-0442(2004)017<1247:IOCFOT>2.0.CO;2.

Wang, J., and Coauthors, 2016: Amazon boundary layer aerosol concentration sustained by vertical transport during rainfall. Nature, **539**, 416–419, https://doi.org/10.1038/nature19819.

Wang, M., and J. Penner, 2009: Aerosol indirect forcing in a global model with particle nucleation. Atmos. Chem. Phys., **9**, 239–260, https://doi.org/10.5194/acp-9-239-2009.

Wendisch, M., and Coauthors, 2016: The ACRIDICON-CHUVA campaign: Studying tropical deep convective clouds and precipitation over Amazonia using the new German research aircraft HALO. Bull. Amer. Meteor. Soc., **97**, 1885–1908, https://doi.org/10.1175/BAMS-D-14-00255.1.

Winker, D., J. Pelon, and M. Mccormick, 2003: The CALIPSO mission: Spaceborne lidar for observation of aerosols and clouds. Proc. SPIE, **4893**, https://doi.org/10.1117/12.466539.

——, M. Vaughan, A. Omar, Y. Hu, K. Powell, Z. Liu, W. Hunt, and S. Young, 2009: Overview of the CALIPSO mission and CALIOP data processing algorithms. J. Atmos. Oceanic Technol., **26**, 2310–2323, https://doi.org/10.1175/2009JTECHA1281.1.

Xavier, T. M. B. S., A. F. S. Xavier, P. L. S. Dias, and M. A. F. S. Dias, 2000: A Zona de Convergência Intertropical – ZCIT e suas relações com a chuva no Ceará. Rev. Bras. Meteor., **15**, 27–43.

Yáñez-Serrano, A. M., and Coauthors, 2020: Amazonian biogenic volatile organic compounds under global change. Global Change Biol., **26**, 4722–4751, https://doi.org/10.1111/gcb.15185.

Yu, F., and G. Luo, 2009: Simulation of particle size distribution with a global aerosol model: Contribution of nucleation to aerosol and CCN number concentrations. Atmos. Chem. Phys., **9**, 7691–7710, https://doi.org/10.5194/acp-9-7691-2009.

Yu, P., O. B. Toon, R. R. Neely, B. G. Martinsson, and C. A. M. Brenninkmeijer, 2015: Composition and physical properties of the Asian tropopause aerosol layer and the North American tropospheric aerosol layer. Geophys. Res. Lett., **42**, 2540–2546, https://doi.org/10.1002/2015GL063181.

Zhou, J., and K.-M. Lau, 1998: Does a monsoon climate exist over South America? J. Climate, **11**, 1020–1040, https://doi.org/10.1175/1520-0442(1998)011<1020:DAMCEO>2.0.CO;2.